Korea-Australia Rheology Journal
Vol. 13, No. 2, June 2001 pp. 97-106

Three dimensional flow analysis within a profile extrusion die by using control volume finite-element method

Jongman Kim, Jae Ryoun Youn* and Jae Chun Hyun[1]
School of Materials Science and Engineering, Seoul National University, Seoul 151-742, Korea
[1]Department of Chemical Engineering, Korea University, Seoul 136-701, Korea
(Received March 5, 2001; final revision received May 16, 2001)

Abstract

Three-dimensional flow analysis was performed by using the control volume finite-element method for design of a profile extrusion die. Because polymer melt behavior is complicated and cross-sectional shape of the profile extrusion die is changing continuously, the fluid flow within the die must be analyzed three-dimensionally. A commercially available polypropylene is used for theoretical and experimental investigations. Material properties are assumed to be constant except for the viscosity. The 5-constant modified Cross model is used for the numerical analysis. A test problem is examined in order to verify the accuracy of the numerical method. Simulations are performed for conditions of three different screw speeds and three different die temperatures. Predicted pressure distribution is compared with the experimental measurements and the results of the previous two-dimensional study. The computational results obtained by using three dimensional CVFEM agree with the experimental measurements and are more accurate than those obtained by using the two-dimensional cross-sectional method. The velocity profiles and the temperature distributions within several cross-sections of the die are given as contour plots.

Keywords : profile extrusion die, CVFEM, 5-constant modified Cross model, three-dimensional numerical simulation

1. Introduction

Extrusion is one of the main processing methods for production of thermoplastic parts. It is used to manufacture pipes, films, fibers, cables, wires, and various continuous profiles. It has an advantage because products are made continuously with lower cost. The screw and extrusion die are the most important parts in the extruder. This study concentrated on melt flow within the die channel for understanding of flow behavior in a profile extrusion die.

Design of a satisfactory extrusion die is a difficult and critical matter. Although some principles are well established and the behavior of polymer melts in constricted channels is understood deeply, there remains a problem of design and construction that relies on experience and art (Morton-Jones, 1989). The profiling of the transition zone is an important problem in the design of profile extrusion dies. The undesirable change in geometry may result in the stagnation of polymer melts. Large residence times by stagnation may lead to thermal degradation of the polymer melt and this can create defects in the final product.

For a good design of the die, flow distribution within the die channel must be identified for a given geometry. Because the polymer melt behavior is not simple and the cross-sectional shape of the die is quite complex, numerical simulations have been used for design of the extrusion die. There are many studies where various numerical analyses are carried out for the design of the profile extrusion die. In the case of two dimensional numerical simulation, the flow analysis network (FAN) method that is based on analytical calculation of the pressure drop and flow rate has been proposed (Tadmor and Broyer, 1974; Lee, 1990), and the cross-sectional method, which considered two dimensional cross sections perpendicular to the flow direction, has been performed (Hurez and Tanguy, 1993; Seo and Youn, 2000). Three dimensional numerical analysis is recently proposed for better precision (Baliga and Patankar, 1988; Kihara *et al.*, 1999; Lee and Yang, 2000).

Because the polymer melt has low thermal conductivity, the convective contribution is predominant in the flow. Conventional Galerkin finite element methods could produce oscillatory solutions at high Peclet numbers. When the convection term is larger than the diffusion term in the momentum equation or energy equation, unrealistic solutions could be obtained. To overcome physically unrealistic

*Corresponding author: jaeryoun@gong.snu.ac.kr

oscillatory solutions, several upwind type finite element methods have been proposed. Heinrich *et al.* (1977), Huyakorn (1977), Hughes *et al.* (1979), and Baliga and Patankar (1980) proposed upwind type finite element methods for convection diffusion problems. Swaminatha and Voller (1992) compared the streamline upwind Petrov Galerkin (SUPG) finite element approach with the streamline upwind control volume (SUCV) finite element method. The basic concept of the SUPG approach was extended to the control volume finite element method.

In this study, three dimensional numerical simulation using the control volume finite element method (CVFEM) is proposed. Baliga and Patankar (1980 and 1983) introduced CVFEM for incompressible fluid in an effort to combine the desirable features of CVFDM and FEM. CVFEMs complement and enhance the conventional Galerkin finite element methods. Prakash (1986) and Hookey and Baliga (1988) have proposed CVFEM for incompressible fluid flow.

CVFEM is a general numerical method for the solution of convection diffusion problems. CVFEM can handle irregular shaped and multiply connected domains and can give accurate solutions over all range of Peclet numbers. The purpose of the convection-diffusion problem is to obtain the distribution of a scalar quantity in the presence of a fluid flow. The scalar quantity is convected with the flow and diffused by its gradients. Therefore, the calculation of the fluid flow must be formerly considered for solving of the convection-diffusion problem. In CVFEM, the shape function is exponential in the direction of the average velocity vector and linear in the normal direction over each element. As this exponential shape function is used, the solution in convection diffusion problem can avoid the physically unrealistic oscillation and false diffusion. To avoid a checker-board pressure problem, two methods are used in CVFEM. in one method, velocity components are computed at all the grid points in the domain and pressure is computed at much fewer grid points. In the other method, velocity and pressure are computed at all the grid points in the domain by using the particular shape function which accounts explicitly for the source terms. The latter method is used in this study.

As the viscosity of polymer melt is sensitive to temperature, the temperature distribution within the die needs to be calculated. To determine the boundary conditions for solving the temperature field in the polymer melt, the temperature distribution in the solid die is calculated. Considering the extrusion head and the die as a cylinder, three dimensional heat transfer problem is changed into two dimensional numerical problem (Seo and Youn, 2000). The modified Cross model is used as the viscosity model. Because the pressure difference within the die is small, effect of pressure on the viscosity is neglected. Four constants of the modified Cross model were determined to fit the data obtained by RMS (Rheometric Mechanical Spectrometer). To verify the computer code, a test problem that has a known solution is solved by the CVFEM. The simulation results of the fluid flow within the die are compared with the experimental results and the two dimensional simulation results reported by Seo and Youn (2000).

2. Theoretical modeling

In the profile extrusion die, the cross-sectional shape is changing continuously and three dimensional computation will yield more accurate prediction than two dimensional analysis. For three dimensional numerical simulation, governing equations are shown in this section and the method for the calculation of the temperature distribution in the solid die is explained. To solve the energy equation for the fluid flow within the die, the wall boundary conditions are required.

2.1. Governing equations

In order to predict the fluid flow of polymer melt within the die, following assumptions were made.

1. The polymer melt is an incompressible Generalized Newtonian Fluid (GNF).
2. The gravitational force is neglected.
3. The flow within the die is in steady state.
4. Creeping flow is assumed within the die because the inertia force is much smaller than the viscous force.

In the Cartesian coordinate system, the fluid flow and heat transfer problems are governed by the following differential equations.

continuity equation:

$$\frac{\partial u}{\partial x}+\frac{\partial v}{\partial y}+\frac{\partial w}{\partial z}=0 \tag{1}$$

momentum equation in x-direction:

$$-\frac{\partial p}{\partial x}+2\frac{\partial}{\partial x}\left(\eta\frac{\partial u}{\partial x}\right)+\frac{\partial}{\partial y}\left(\eta\frac{\partial v}{\partial x}+\eta\frac{\partial u}{\partial y}\right)+\frac{\partial}{\partial z}\left(\eta\frac{\partial w}{\partial x}+\eta\frac{\partial u}{\partial z}\right)=0 \tag{2}$$

momentum equation in y-direction:

$$-\frac{\partial p}{\partial y}+\frac{\partial}{\partial x}\left(\eta\frac{\partial u}{\partial y}+\eta\frac{\partial v}{\partial x}\right)+2\frac{\partial}{\partial y}\left(\eta\frac{\partial v}{\partial y}\right)+\frac{\partial}{\partial z}\left(\eta\frac{\partial w}{\partial y}+\eta\frac{\partial v}{\partial z}\right)=0 \tag{3}$$

momentum equation in z-direction:

$$-\frac{\partial p}{\partial z}+\frac{\partial}{\partial x}\left(\eta\frac{\partial u}{\partial z}+\eta\frac{\partial w}{\partial x}\right)+\frac{\partial}{\partial y}\left(\eta\frac{\partial v}{\partial z}+\eta\frac{\partial w}{\partial y}\right)+2\frac{\partial}{\partial z}\left(\eta\frac{\partial w}{\partial z}\right)=0 \tag{4}$$

energy equation:

$$\rho C_p\left(\frac{\partial}{\partial x}(uT)+\frac{\partial}{\partial y}(vT)+\frac{\partial}{\partial z}(wT)\right)-\frac{\partial}{\partial x}\left(k\frac{\partial T}{\partial x}\right)-\frac{\partial}{\partial y}\left(k\frac{\partial T}{\partial y}\right)-\frac{\partial}{\partial z}\left(k\frac{\partial T}{\partial z}\right)$$

$$=2\eta\left(\frac{\partial u}{\partial x}\right)^2+2\eta\left(\frac{\partial v}{\partial y}\right)^2+2\eta\left(\frac{\partial w}{\partial z}\right)^2+\eta\left(\frac{\partial u}{\partial y}\right)^2+\eta\left(\frac{\partial v}{\partial x}\right)^2+\eta\left(\frac{\partial v}{\partial z}\right)^2$$

$$+\eta\left(\frac{\partial w}{\partial y}\right)^2+\eta\left(\frac{\partial w}{\partial x}\right)^2+\eta\left(\frac{\partial u}{\partial z}\right)^2+2\eta\frac{\partial u}{\partial y}\frac{\partial v}{\partial x}+2\eta\frac{\partial v}{\partial z}\frac{\partial w}{\partial y}+2\eta\frac{\partial u}{\partial z}\frac{\partial w}{\partial x} \quad (5)$$

In the above equations, ρ is the density of the fluid, C_p heat capacity, η viscosity of the fluid, k thermal conductivity, p hydraulic pressure, T temperature, and u, v, and w are the velocity components in x, y, and z directions.

The constitutive equation is important to obtain the acceptable numerical result and the modified Cross model was selected. The 5-constant model is described as follows:

$$\eta=\frac{\eta_0(T,p)}{1+(\eta_0\dot{\gamma}/\tau^*)^{1-n}} \quad (6)$$

$$\eta_0(T,p)=B\exp\left(\frac{T_b}{T}\right)\exp(\beta p) \quad (7)$$

where τ^*, B, T_b, β and n are the model parameters, η_0 zero shear viscosity and $\dot{\gamma}$ the shear rate defined as follows:

$$\dot{\gamma}=\sqrt{(\dot{\gamma}_{ij}\dot{\gamma}_{ij})/2} \quad (8)$$

$$\dot{\gamma}_{ij}=v_{i,j}+v_{j,i} \quad (9)$$

2.2. Temperature distribution in the solid die

When the energy equation (5) is calculated, boundary conditions at the solid wall should be known. The temperature distribution in the solid die was calculated by the finite element method. For the accurate calculation, a three dimensional heat transfer problem must be considered. However, since the die was assumed as a cylinder, it became a two dimensional heat transfer problem (Fig. 1). To compute the temperature in the solid die, the temperature in the extruder head must be considered because the temperature of extruder head affects the temperature distribution in the solid die. When the temperature distribution in the solid die was calculated, the following assumptions were used.

1. Nothing is attached to the solid die.
2. The polymer melt within the die is stationary.
3. The heat supply from the heater is continuous.

In practice, the heater, regularly supplying the heat, is attached to the solid die and the polymer melt advances due to pressure gradient in the die. By using the above assumptions, the heat conduction equation was taken into account for the solution. Details for the calculation of temperature distribution in the solid die are described by the previous study (Seo and Youn, 2000).

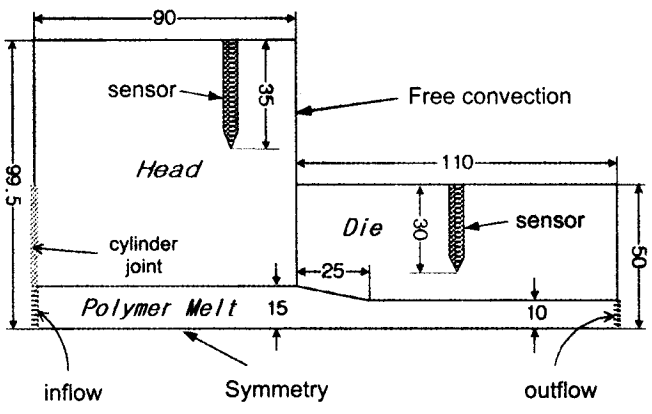

Fig. 1. Schematic diagram of the die head and die channel.

3. Numerical analysis

3.1. Control volume finite element method

Control volume finite element method has been used for three dimensional heat transfer and fluid flow problems (Baliga and Patankar, 1988). In numerical methods based on the formulation of primitive variables, the resulting discretization equations could admit checkerboard type pressure fields, if the velocity components and pressure are stored at the same grid points and interpolated by similar functions. To avoid this difficulty, an unequal-order CVFEM (Baliga and Patankar, 1983) and an equal-order CVFEM (Prakash, 1986) have been proposed. The present study is based on the latter suggested by Prakash.

3.1.1. Domain discretization

The four noded tetrahedron is used as a basic discretized element. After the discretization of the calculation domain with four-node tetrahedral elements, each node is associated with a polyhedral control volume generated as follows. The center of each tetrahedral element is first joined by straight lines to the center of the four triangular surfaces that make the tetrahedron. Then, straight lines to the midpoints of the corresponding sides join the center of each triangular surface. This procedure generates six quadrilateral planar surfaces within each tetrahedral element. The surfaces divide the tetrahedral element into four equal, but not necessarily similar shaped, volumes as shown in Fig. 2.

3.1.2. Control volume conservation equations

Steady, three dimensional, elliptic convection diffusion phenomena are governed by differential equations that can be cast in the following general form.

$$div(\boldsymbol{J})=S_\phi \quad (10)$$

$$\boldsymbol{J}=\rho v\phi-\Gamma_\phi\nabla\phi \quad (11)$$

where ϕ is a general scalar dependent variable, ρ the mass density, v the fluid velocity vector, Γ_ϕ the diffusion coefficient, S_ϕ the volumetric source term, and $\boldsymbol{J}$ the combined convection and diffusion flux of ϕ.

An integral formulation corresponding to equation (10) can be obtained by applying the conservation principle for ϕ to a control volume V, which is fixed in space. The resulting integral conservation equation, when applied to the polyhedral control volume surrounding the node 1 of

$$+\eta\left(\frac{\partial w}{\partial y}\right)^2+\eta\left(\frac{\partial w}{\partial x}\right)^2+\eta\left(\frac{\partial u}{\partial z}\right)^2+2\eta\frac{\partial u}{\partial y}\frac{\partial v}{\partial x}+2\eta\frac{\partial v}{\partial z}\frac{\partial w}{\partial y}+2\eta\frac{\partial u}{\partial z}\frac{\partial w}{\partial x} \quad (5)$$

In the above equations, ρ is the density of the fluid, C_p heat capacity, η viscosity of the fluid, k thermal conductivity, p hydraulic pressure, T temperature, and u, v, and w are the velocity components in x, y, and z directions.

The constitutive equation is important to obtain the acceptable numerical result and the modified Cross model was selected. The 5-constant model is described as follows:

$$\eta=\frac{\eta_0(T,p)}{1+(\eta_0\dot{\gamma}/\tau^*)^{1-n}} \quad (6)$$

$$\eta_0(T,p)=B\exp\left(\frac{T_b}{T}\right)\exp(\beta p) \quad (7)$$

where τ^*, B, T_b, β and n are the model parameters, η_0 zero shear viscosity and $\dot{\gamma}$ the shear rate defined as follows:

$$\dot{\gamma}=\sqrt{(\dot{\gamma}_{ij}\dot{\gamma}_{ij})/2} \quad (8)$$

$$\dot{\gamma}_{ij}=v_{i,j}+v_{j,i} \quad (9)$$

2.2. Temperature distribution in the solid die

When the energy equation (5) is calculated, boundary conditions at the solid wall should be known. The temperature distribution in the solid die was calculated by the finite element method. For the accurate calculation, a three dimensional heat transfer problem must be considered. However, since the die was assumed as a cylinder, it became a two dimensional heat transfer problem (Fig. 1). To compute the temperature in the solid die, the temperature in the extruder head must be considered because the temperature of extruder head affects the temperature distribution in the solid die. When the temperature distribution in the solid die was calculated, the following assumptions were used.

1. Nothing is attached to the solid die.
2. The polymer melt within the die is stationary.
3. The heat supply from the heater is continuous.

In practice, the heater, regularly supplying the heat, is attached to the solid die and the polymer melt advances due to pressure gradient in the die. By using the above assumptions, the heat conduction equation was taken into account for the solution. Details for the calculation of temperature distribution in the solid die are described by the previous study (Seo and Youn, 2000).

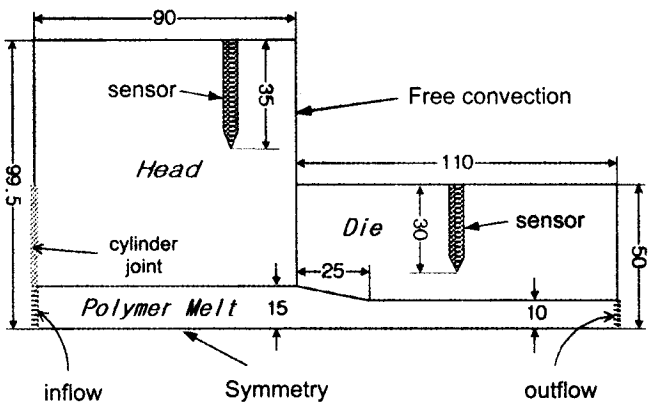

Fig. 1. Schematic diagram of the die head and die channel.

3. Numerical analysis

3.1. Control volume finite element method

Control volume finite element method has been used for three dimensional heat transfer and fluid flow problems (Baliga and Patankar, 1988). In numerical methods based on the formulation of primitive variables, the resulting discretization equations could admit checkerboard type pressure fields, if the velocity components and pressure are stored at the same grid points and interpolated by similar functions. To avoid this difficulty, an unequal-order CVFEM (Baliga and Patankar, 1983) and an equal-order CVFEM (Prakash, 1986) have been proposed. The present study is based on the latter suggested by Prakash.

3.1.1. Domain discretization

The four noded tetrahedron is used as a basic discretized element. After the discretization of the calculation domain with four-node tetrahedral elements, each node is associated with a polyhedral control volume generated as follows. The center of each tetrahedral element is first joined by straight lines to the center of the four triangular surfaces that make the tetrahedron. Then, straight lines to the midpoints of the corresponding sides join the center of each triangular surface. This procedure generates six quadrilateral planar surfaces within each tetrahedral element. The surfaces divide the tetrahedral element into four equal, but not necessarily similar shaped, volumes as shown in Fig. 2.

3.1.2. Control volume conservation equations

Steady, three dimensional, elliptic convection diffusion phenomena are governed by differential equations that can be cast in the following general form.

$$div(\boldsymbol{J})=S_\phi \quad (10)$$

$$\boldsymbol{J}=\rho v\phi-\Gamma_\phi\nabla\phi \quad (11)$$

where ϕ is a general scalar dependent variable, ρ the mass density, v the fluid velocity vector, Γ_ϕ the diffusion coefficient, S_ϕ the volumetric source term, and $\boldsymbol{J}$ the combined convection and diffusion flux of ϕ.

An integral formulation corresponding to equation (10) can be obtained by applying the conservation principle for ϕ to a control volume V, which is fixed in space. The resulting integral conservation equation, when applied to the polyhedral control volume surrounding the node 1 of

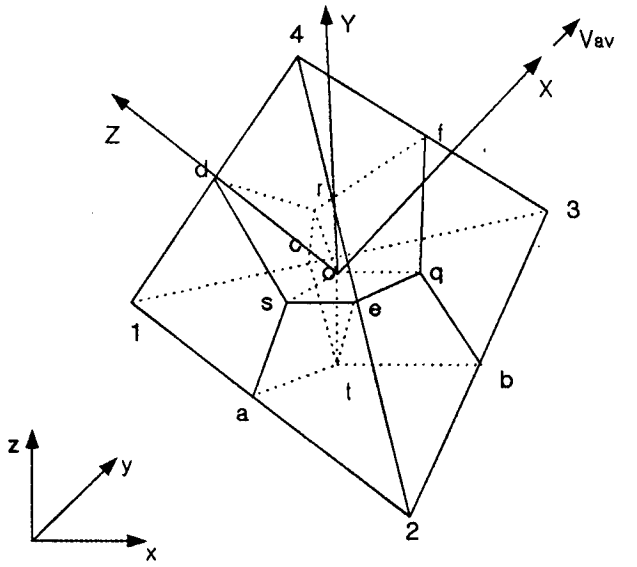

Fig. 2. Division of a tetrahedral element into portions of polyhedral control volumes and local flow-oriented *X*, *Y*, *Z* and global *x*, *y*, *z* coordinate systems.

the tetrahedral element shown in Fig. 2, can be expressed in the following form.

$$[\int_{atos} \boldsymbol{J}\cdot\boldsymbol{n}\, ds+\int_{ctor} \boldsymbol{J}\cdot\boldsymbol{n}\, ds+\int_{dsor} \boldsymbol{J}\cdot\boldsymbol{n}\, ds-\int_{atcdsor} S_\phi dV]$$
$$+ \text{ [similar contributions from other elements associated with node 1]}$$
$$+\text{[boundary contributions, if applicable]}=0 \quad (12)$$

The integral equation that expresses the momentum conservation equations and energy balance equation can be obtained from equation (12).

The integral mass conservation equation is also imposed on the polyhedral control volumes. This equation can be written as follows.

$$[\int_{atos} \rho\boldsymbol{v}\cdot\boldsymbol{n}\, ds+\int_{ctor} \rho\boldsymbol{v}\cdot\boldsymbol{n}\, ds+\int_{dsor} \rho\boldsymbol{v}\cdot\boldsymbol{n}\, ds]$$
$$+ \text{ [similar contributions from other elements associated with node 1]}$$
$$+\text{[boundary contributions, if applicable]}=0 \quad (13)$$

The source term and pressure is interpolated linearly in each element. The interpolation function is defined with respect to a local flow-oriented Cartesian coordinate system (*X*, *Y*, *Z*), shown in Fig. 2. Algebraic approximations of the internal contributions and boundary contributions are derived for all elements in the calculation domain. When approximations of the contributions from all the elements associated with a typical node *i* are substituted into equation (12), the corresponding discretization equation is obtained. This equation can be expressed in the following general form:

$$a_i^\phi \phi_i = \sum_n a_n^\phi \phi_n + b_i^\phi \quad (14)$$

where the summation is taken over all neighbors of node i. When the value of ϕ at a node i is specified the corresponding discretization equation becomes the following trivial form like a specified boundary condition:

$$\phi_i = \phi_{specified} \quad (15)$$

Details of the derivations are given in the reference (Baliga and Patankar, 1988).

3.2. Formulation for the flow within the die

3.2.1. Formulation for the fluid flow

The fluid flow problem is governed by the momentum equations (2) to (4). Because the fluid flow is assumed as the creeping flow, the convection term is neglected. Therefore, the fluid flow is three-dimensional conduction type problem (Baliga and Patankar, 1988). For the conduction type problem, the general form of flux is written as the following form:

$$J = -\Gamma_\phi \nabla\phi \quad (16)$$

For the momentum equations, the flux and the source is expressed as the following form:

For x-momentum equation

$$J = 2\eta\frac{\partial u}{\partial x}i-\eta\left(\frac{\partial v}{\partial x}+\frac{\partial u}{\partial y}\right)j-\eta\left(\frac{\partial w}{\partial x}+\frac{\partial u}{\partial z}\right)k$$
$$S^u = -\frac{\partial p}{\partial x} \quad (17)$$

For y-momentum equation

$$J = -\eta\left(\frac{\partial u}{\partial y}+\frac{\partial v}{\partial x}\right)i-2\eta\frac{\partial v}{\partial y}j-\eta\left(\frac{\partial w}{\partial y}+\frac{\partial v}{\partial z}\right)k$$
$$S^v = -\frac{\partial p}{\partial y} \quad (18)$$

For z-momentum equation

$$J = -\eta\left(\frac{\partial u}{\partial z}+\frac{\partial w}{\partial x}\right)i-\eta\left(\frac{\partial v}{\partial z}+\frac{\partial w}{\partial y}\right)j-2\eta\frac{\partial w}{\partial z}k$$
$$S^w = -\frac{\partial p}{\partial z} \quad (19)$$

where the pressure gradient is considered as the source and the viscosity, η is calculated by equations (6), (7), and (10). As the convection term is neglected, the global Cartesian coordinate system (*x*, *y*, *z*) is used instead of the local flow oriented Cartesian coordinate system (*X*, *Y*, *Z*) for the interpolation function. Then, the interpolation functions are given as follows:

$$u = A^u x+B^u y+C^u z+D^u-\frac{1}{\eta}\frac{\partial p}{\partial x}\left[x-\frac{1}{4}(y^2+z^2)\right] \quad (20)$$

$$v = A^v x + B^v y + C^v z + D^v - \frac{1}{\eta}\frac{\partial p}{\partial y}\left[y - \frac{1}{4}(z^2 + x^2)\right] \quad (21)$$

$$w = A^w x + B^w y + C^w z + D^w - \frac{1}{\eta}\frac{\partial p}{\partial z}\left[z - \frac{1}{4}(x^2 + y^2)\right] \quad (22)$$

The equations (20) to (22) satisfy the equations (2) to (4), respectively.

Using Gaussian quadrature approximation, the resulting u, v, and w discretization equations for node i can be expressed as follows:

$$a_i^u u_i = \sum_n a_n^u u_n + d_i^u + \sum_n \Omega_n^u p_n \quad (23)$$

$$a_i^v v_i = \sum_n a_n^v v_n + d_i^v + \sum_n \Omega_n^v p_n \quad (24)$$

$$a_i^w w_i = \sum_n a_n^w w_n + d_i^w + \sum_n \Omega_n^w p_n \quad (25)$$

Using guessed values of u, v, w, and p, or values from a previous cycle of an iterative solution procedure, the coefficients in equations (23) to (25) can be calculated, and these equations can be solved to obtain new values of u, v, and w using the SIMPLEC procedure (Baliga and Patankar, 1983).

3.2.2. Formulation for the heat transfer

The heat transfer problem is governed by the equation (5). Because the problem is a convection-diffusion type, the local flow oriented Cartesian coordinate (X, Y, Z) is used. With the equations (5), (10), and (11), the heat flux and the source term can be expressed as follows:

$$J = \left(\rho C_p UT - k\frac{\partial T}{\partial X}\right)i + \left(\rho C_p VT - k\frac{\partial T}{\partial Y}\right)j + \left(\rho C_p WT - k\frac{\partial T}{\partial Z}\right)k,$$

$$S_T = 2\eta\left(\frac{\partial U}{\partial X}\right)^2 + 2\eta\left(\frac{\partial V}{\partial Y}\right)^2 + 2\eta\left(\frac{\partial W}{\partial Z}\right)^2 + \eta\left(\frac{\partial U}{\partial Y}\right)^2 + \eta\left(\frac{\partial V}{\partial X}\right)^2$$
$$+ \eta\left(\frac{\partial V}{\partial Z}\right)^2 + \eta\left(\frac{\partial W}{\partial Y}\right)^2 + \eta\left(\frac{\partial W}{\partial X}\right)^2 + \eta\left(\frac{\partial U}{\partial Z}\right)^2$$
$$+ 2\eta\frac{\partial U}{\partial Y}\frac{\partial V}{\partial X} + 2\eta\frac{\partial V}{\partial Z}\frac{\partial W}{\partial Y} + 2\eta\frac{\partial U}{\partial Z}\frac{\partial W}{\partial X} \quad (26)$$

An interpolation function for temperature must satisfy the convection diffusion equation, respond appropriately to the direction of V_{av}, represent the value of the element based Peclet number, and account for the influence of the source term explicitly. The temperature interpolation function is given by the following;

$$T = A^T\xi + B^T Y + C^T Z + D^T + S_T\left[\frac{X}{N\rho C_p U_{av}} - \frac{1 - 1/N}{4k}(Y^2 + Z^2)\right] \quad (27)$$

Using Gaussian quadrature, the resulting temperature discretization equations for node i can be expressed as follows;

$$a_i^T T_i = \sum_n a_n^T T_n + b_i^T \quad (28)$$

where the summation is taken over all neighbors of node i.

In the iterative solution of the algebraic equations, it is often desirable to slow down the changes, from iteration to iteration, in the values of the dependent variable (Patankar, 1980). This process is called underrelaxation. Underrelaxation is a very useful device for nonlinear problems. It may be employed to avoid divergence in the iterative solution and was used for solving the discretization equations (23), (24), (25), and (28). The procedure for numerical simulation is shown succinctly in Fig. 3.

3.3. Test problem

To verify the computer built code used for the numerical analysis, a test problem was performed. Flow of a Newtonian fluid within a circular cylinder was used as the test problem. Considering the geometrical symmetry, a quarter of the cylinder cross-section was used for the numerical analysis. Because an exact analytical solution exists for this problem, the validation of the code can be made by comparing the numerical solution with the exact solution. When the pressure difference is fixed, the pressure along the flow direction is shown in Fig. 4 and the velocity for the flow direction along the radius is shown in Fig. 5. The solid line indicates the results of the numerical analysis and the dashed line indicates the analytical solution in Figs. 4 and 5. There is a good agreement between the numerical results and the analytical solution. Maximum error in the velocity distribution is only 2%. In the case of the pressure distri-bution, the error is quite small.

4. Results and discussion

A commercial polypropylene was used as the material for the numerical analysis and experimental investigations. Material properties are given in Table 1. Constants of the viscosity model are given in the reference (Seo and Youn, 2000). Because the shear rate was low for the flow in the profile extrusion die, RMS was used for the measurement of the viscosity. In the range of shear rate for the profile extrusion, the viscosity predicted by the 5-constant modified Cross model shows a good agreement with the experimental data.

The geometry of the L-shape profile extrusion die used for the simulation and the experiment is shown in Fig. 6(a) and a part of the three dimensional finite element mesh is presented in Fig. 6(b). In order to compare the experimental results with the previous work, the conditions of the study by Seo and Youn (2000) were used for the simulation. For the screw speed, 30, 60, and 90 rpm were used, and for the die temperature, 453, 473, and 493 K were used. The head temperature was assumed to be 473 K. A total of 2406 nodes and 10729 elements were used for the

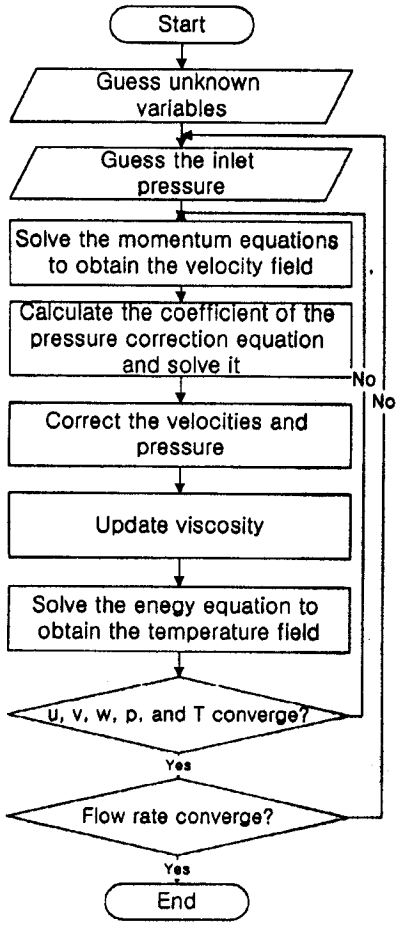

Fig. 3. Flow chart for the numerical calculation.

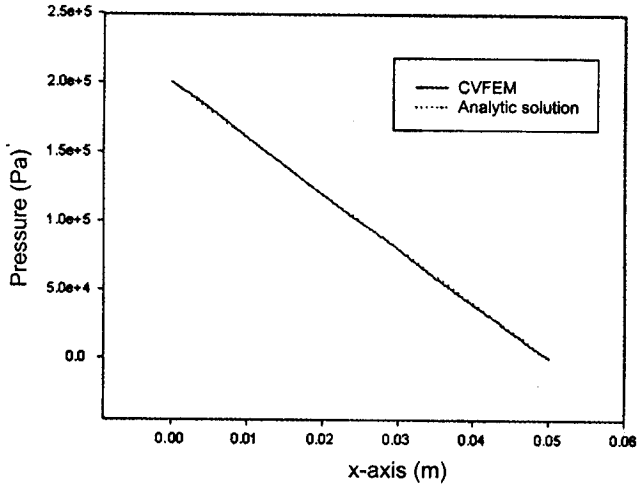

Fig. 4. Pressure variation of the polymer melts along the die channel for the test problem.

die. The flow rate does not depend on the temperature but is dependent on the screw speed. According to the results by Seo and Youn (2000), it can be known that the flow rate linearly changes with respect to the screw speed.

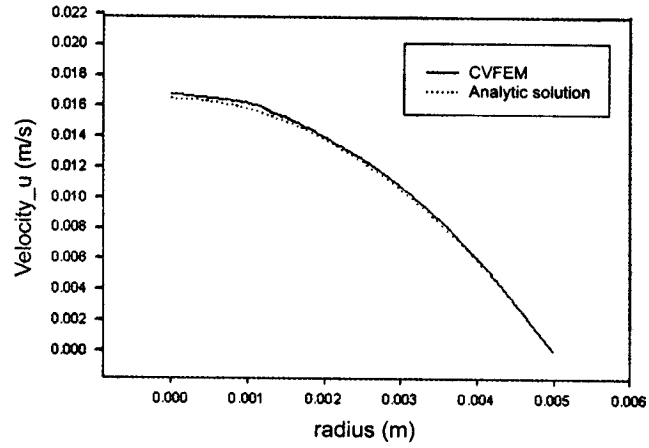

Fig. 5. Variation of the x-direction velocity as a function of the radius for the test problem.

Table 1. Material properties and five constants of the viscosity model

	PP (Hopelen)
Density (kg/m^3)	770
Heat capacity (J/kg · K)	3060
Heat conductivity (W/m · K)	0.151
n	0.342
τ^* (Pa)	7.52E+3
B (Pa · s)	2.36E-2
T_b (K)	5.236E+3
β (Pa^{-1})	1.5E-8

It was assumed that the flow in the inlet of the head was fully developed. At the wall boundary, non-slip condition was used for the velocity and isothermal condition was used for the temperature. The pressure difference between the inlet and the outlet was assumed as an arbitrary value at first, and then the flow rate was calculated by the numerical results obtained from the pressure difference. This process was repeated until the calculated flow rate was equal to the experimentally measured flow rate. To compare the experimental data with the simulation results in each condition, the pressure profiles along the flow direction were compared. The pressure at the outlet was considered to be zero. The location of each pressure sensor in the experiment is shown in Fig. 6(a).

When the flow rate is 1.24 g/s, the pressure profiles at different die temperatures are shown in Figs. 7 to 9. In Figs. 7 to 9, two numerical results, i.e., numerical predictions by using three-dimensional CVFEM and by using two dimensional cross-sectional method are plotted and compared with the experimental results. It is clear that the pressure difference is smaller as the die temperature is increased.

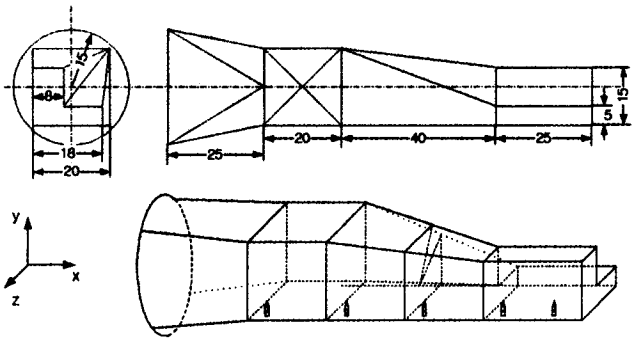

(a)

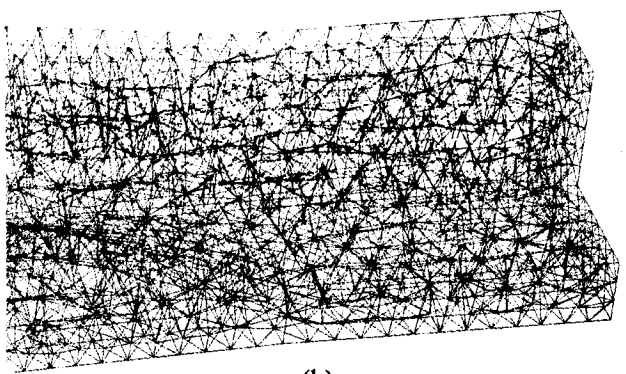

(b)

Fig. 6. (a) Geometry of the L-shape profile extrusion die. (b) A part of the computational mesh

Figs. 8, 10, and 11 show that the flow rate affects pressure difference. As expected, the pressure difference is larger as the flow rate is increased. The simulation results obtained by using three dimensional CVFEM agree well with the experimental measurements and are more accurate than those obtained by using two dimensional cross-sectional method.

The velocity and the temperature profiles in some cross-sections of the die are shown in Figs. 12 to 16. When the flow rate is 1.24 g/s and the die temperature is 473 K, the velocity and the temperature distributions in some cross-sections are obtained. In this case, the temperature distribution along x-axis at the wall boundary is shown in Fig. 12. The velocity and the temperature distributions at 0.095, 0.120, 0.155, and 0.195 m along x-axis are shown in Figs. 13 to 16.

In the case of the symmetric cross-sections as shown in Figs. 13 and 14, the shape of velocity profile is symmetric. But, in the case of asymmetrically shaped cross-sections as shown in Figs. 15 and 16, temperature distributions are rather complex. Because the velocity gradient is small in the die channel, the temperature rise by viscous heating is small and the wall temperature will mainly affect the temperature of the fluid. Therefore, the wall temperature of the solid die must be predicted accurately for calculation of the precise temperature distribution.

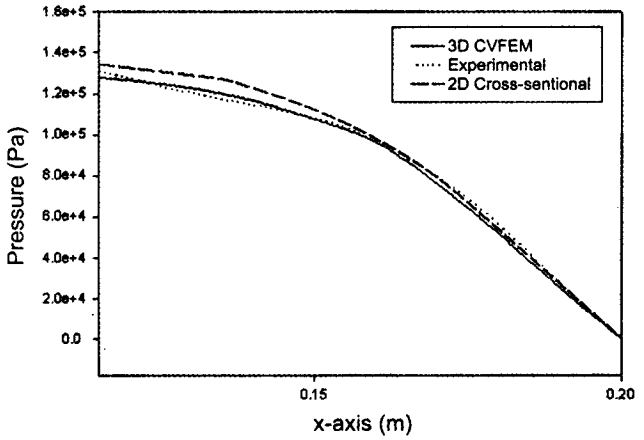

Fig. 8. Pressure variation of the polymer melt along the boundary of the channel in the case of die temperature at 473 K and flow rate of 1.24 g/s.

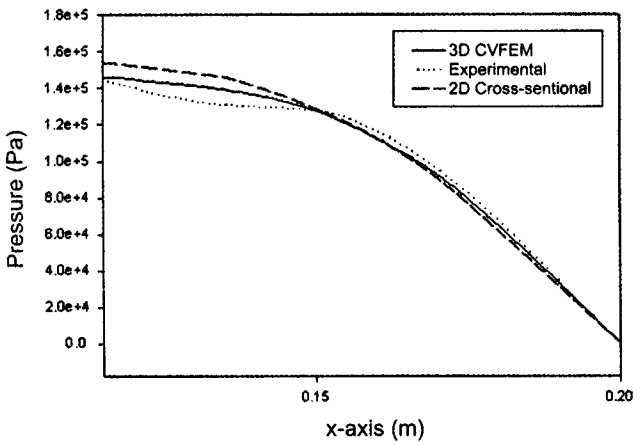

Fig. 7. Pressure variation of the polymer melt along the boundary of the channel in the case of die temperature at 453 K and flow rate of 1.24 g/s.

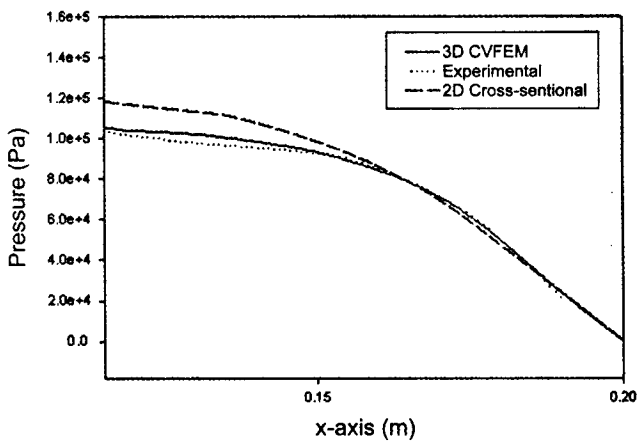

Fig. 9. Pressure variation of the polymer melt along the boundary of the channel in the case of die temperature at 493 K and flow rate of 1.24 g/s.

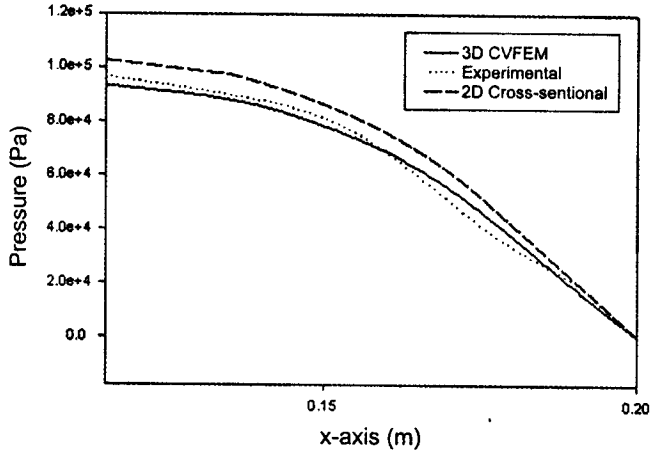

Fig. 10. Pressure variation of the polymer melt along the boundary of the channel in the case of die temperature at 473 K and flow rate of 0.84 g/s.

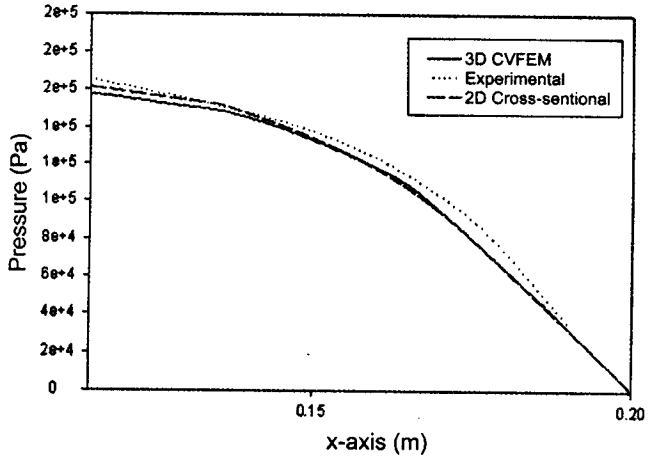

Fig. 11. Pressure variation of the polymer melt along the boundary of the channel in the case of die temperature at 473 K and flow rate of 1.64 g/s.

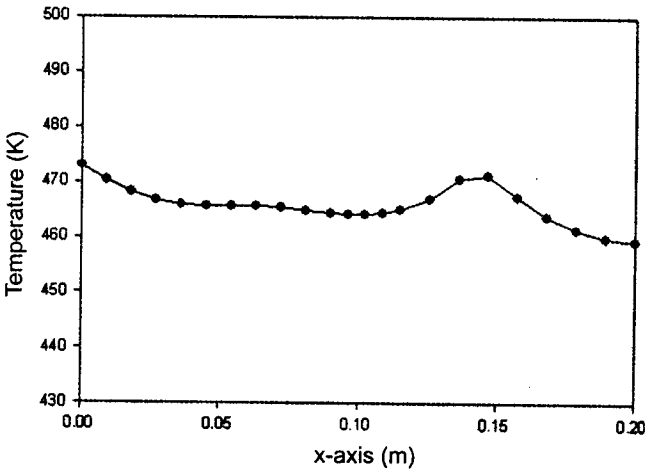

Fig. 12. Temperature distribution at the wall boundary along the die channel.

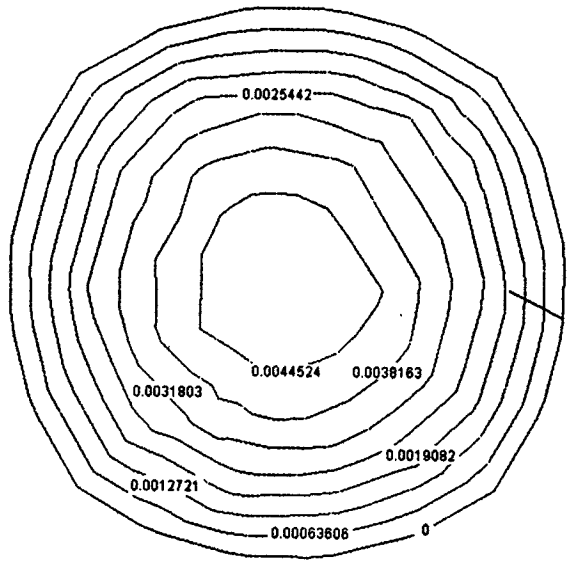

(a)

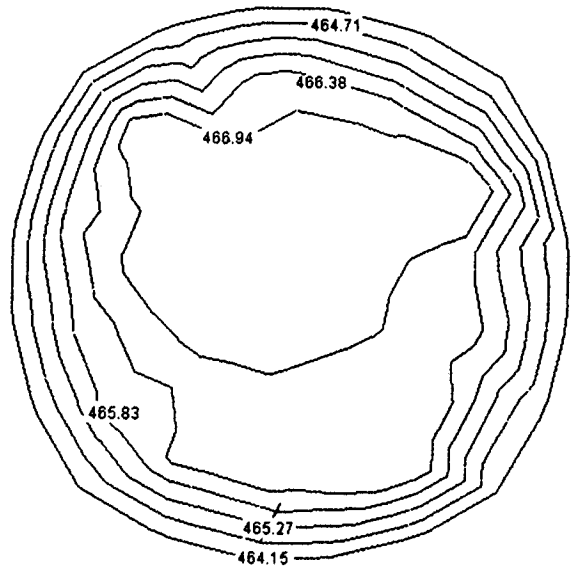

(b)

Fig. 13. Contour plots for die temperature of 473 K and flow rate of 1.24 g/s at x=0.095 m: (a) x-directional velocity (m/s) and (b) temperature (K).

5. Conclusions

The velocity, pressure, and temperature distributions of the fluid flow within the profile extrusion die are calculated by using a three dimensional control volume finite element method. An equal order CVFEM for three dimensional fluid flow problem and a CVFEM for three dimensional heat convection diffusion problem considering viscous heating are formulated. Three dimensional non-isothermal numerical calculation is performed for different screw

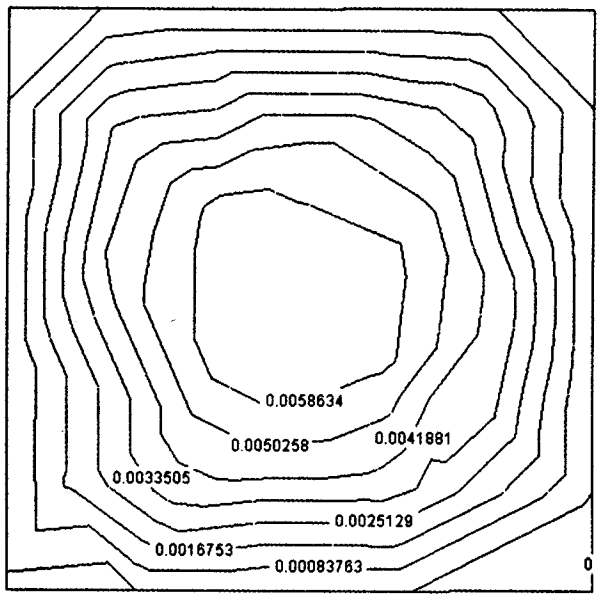

(a)

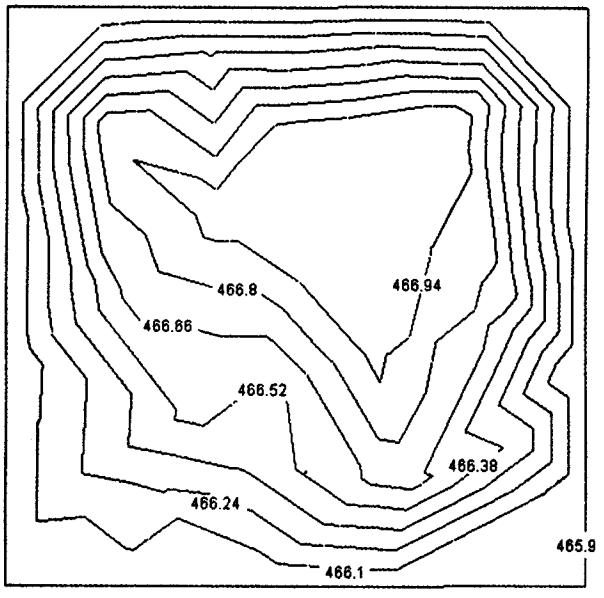

(b)

Fig. 14. Contour plots for die temperature of 473 K and flow rate of 1.24 g/s at x=0.120 m: (a) x-directional velocity (m/s) and (b) temperature (K).

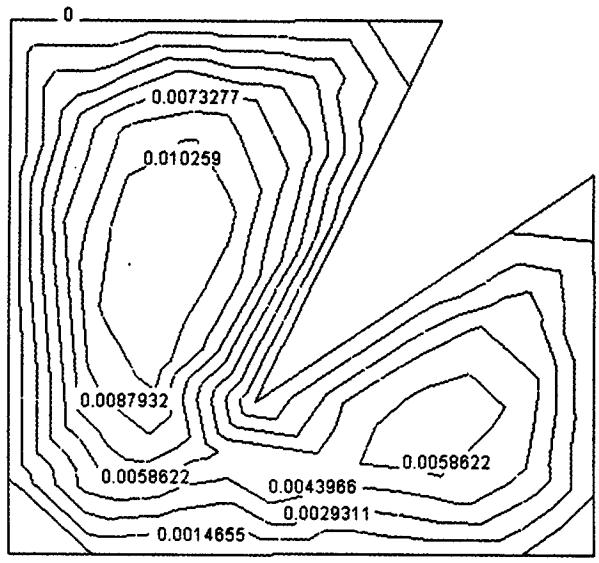

(a)

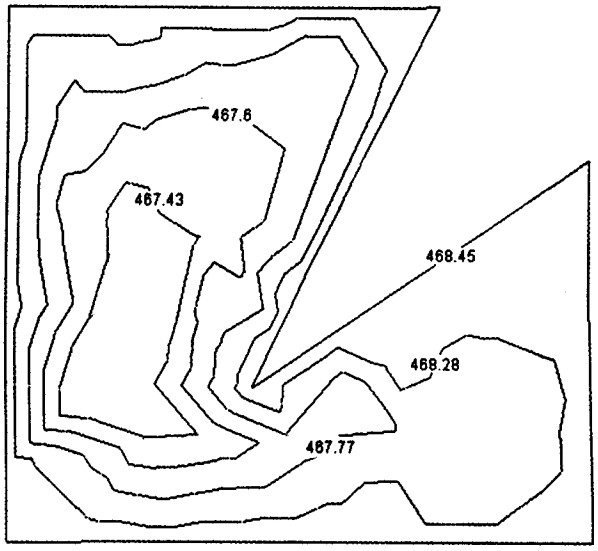

(b)

Fig. 15. Contour plots for die temperature of 473 K and flow rate of 1.24 g/s at x=0.155 m: (a) x-directional velocity (m/s) and (b) temperature (K).

speeds and at different die temperatures. Pressure difference in the die becomes larger as the screw speed is increased, but smaller as the die temperature is increased. Pressure distributions given by the numerical calculations are compared with the experimental measurements and the two-dimensional numerical results for the same profile extrusion die. Simulation results obtained by the three dimensional CVFEM agree well with the experimental results and are more accurate than those obtained by using two dimensional cross-sectional method. Velocity profiles in x direction and temperature distributions at several cross-sections perpendicular to x-axis are given as the contour plots. The results can be utilized for design of the extrusion die and study of the extrudate swell.

Acknowledgement

This study was supported by the research grants from the Korea Science and Engineering Foundation (KOSEF) through the Applied Rheology Center (ARC), an official KOSEF-created engineering research center (ERC) at Korea University, Seoul, Korea.

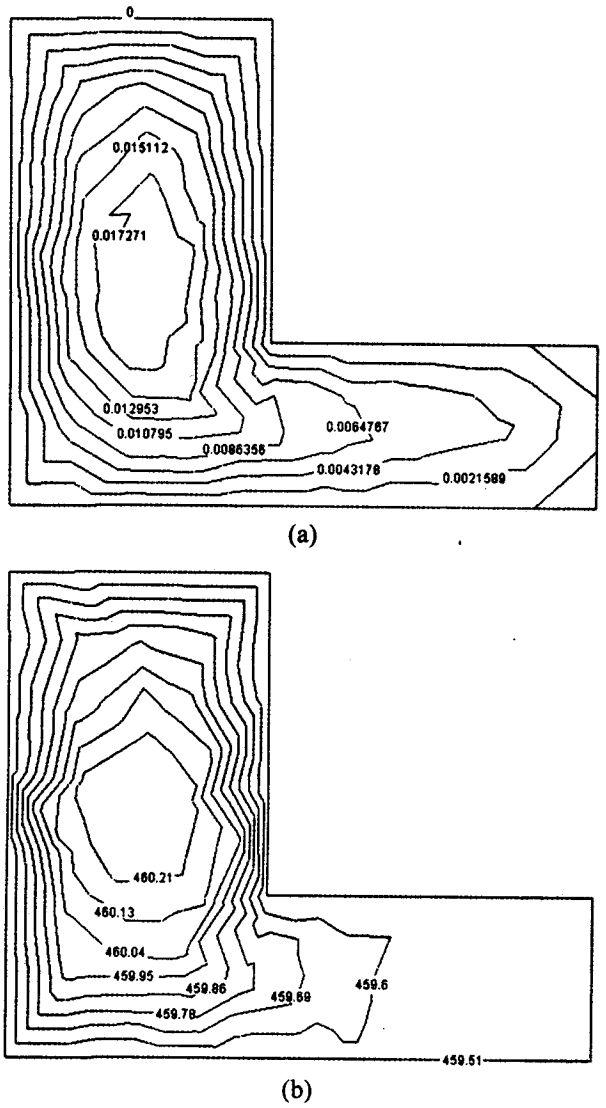

Fig. 16. Contour plots for die temperature of 473 K and flow rate of 1.24 g/s at x=0.195 m: (a) x-directional velocity (m/s) and (b) temperature (K).

References

Baliga, B.R. and S.V. Patankar, 1980, A new finite-element formulatin for convection-diffusion problems, *Numer. heat tr.* **3**, 393.

Baliga, B.R. and S.V. Patankar, 1983, A control volume finite-element method for two-dimensional fluid flow and heat transfer, *Numer. heat tr.* **6**, 245.

Baliga, B.R. and S.V. Patankar, 1988, Handbook of Numerical Heat Transfer, Chap. 11, Elliptic systems: Finite-element method ϕ, Wiley, New York.

Heinrich, J.C., P.S. Huyakorn, O.C. Zienkiewicz and A.R. Mitchell, 1977, An upwind finite element scheme for two-dimensional convective transport equation, *Int. J. Numer. Meth. Eng.* **11**, 131.

Heinrich, J.C., P.S. Huyakorn, O.C. Zienkiewicz and A.R. Mitchell, 1977, Quadratic finite element schemes for two-dimensional convective-transport problem, *Int. J. Numer. Meth. Eng.* **11**, 1831.

Hookey, N.A. and B.R. Baliga, 1988, Evaluation and enhancements of some control volume finite-element method Part 2. Incompressible fluid flow problems, *Numer. heat tr.* **14**, 274.

Hughes, T.J.R., W.K. Liu and A. Brooks, 1979, Review of finite element analysis of incompressible viscous flows by the penalty function formulation, *J. Comp. Phy.* **30**, 1.

Hurez, P. and P.A. Tanguy, 1993, Numerical simulation of profile extrusion dies without flow separation, *Polym. Eng. Sci.* **33**, 971.

Huyakorn, P.S., 1977, Solution to steady-state convective transport equation using an upwind finite element scheme, *Appl. Math. Model.* **1**, 187.

Kihara, S., T. Gouda, K. Matsunaga and K. Funatsu, 1999, Numerical simulation of three-dimensional viscoelastic flow within dies, *Poly. Eng. Sci.* **39**, 152.

Lee, C.C., 1990, An improved flow analysis network (FAN) method for irregular geometries, *Polym. Eng. Sci.* **30**, 1607.

Lee, C.M. and D.Y. Yang, 2000, A three-dimensional steady-state finite element analysis of square die extrusion by using automatic mesh generation, *Int. J. Mach. Tool. Manu.* **40**, 33.

Morton-Jones, D.H., 1989, Polymer Processing, Champman and Hall, New York.

Patankar, S.V., 1980, Numerical heat transfer and fluid flow, Hemisphere, Washington, D.C.

Prakash, C., 1986, An improved control-volume finite-element method for heat and mass transfer and for fluid flow using equal-order velocity-pressure interpolation, *Numer. heat tr.* **9**, 253.

Seo, D. and J.R. Youn, 2000, Flow analysis of profile extrusion by a modified cross-sectional numerical method, *Fibers and Poymers*, **1**, 103.

Swanminathan, C.R. and V. R. Voller, 1992, Streamline upwind scheme for control-volume finite elements Part 1. Formulation, *Numer. heat tr. Part B* **22**, 95.

Tadmor, Z. and E. Broyer, 1974, Flow analysis network (FAN) A method for solving flow problems in polymer processing, *Polym. Eng. Sci.* **14**, 660.